Idle State Classification using Spiking Activity and Local Field Potentials in a Brain Computer Interface

Jordan J. Williams[1], Rex. N. Tien[2], Yoh Inoue[3], and Andrew B. Schwartz[4]

Abstract— **Previous studies of intracortical brain-computer interfaces (BCIs) have often focused on or compared the use of spiking activity and local field potentials (LFPs) for decoding kinematic movement parameters. Conversely, using these signals to detect the initial intention to use a neuroprosthetic device or not has remained a relatively understudied problem. In this study, we examined the relative performance of spiking activity and LFP signals in detecting discrete state changes in attention regarding a user's desire to actively control a BCI device. Preliminary offline results suggest that the beta and high gamma frequency bands of LFP activity demonstrated a capacity for discriminating idle/active BCI control states equal to or greater than firing rate activity on the same channel. Population classifier models using either signal modality demonstrated an indistinguishably high degree of accuracy in decoding rest periods from active BCI reach periods as well as other portions of active BCI task trials. These results suggest that either signal modality may be used to reliably detect discrete state changes on a fine time scale for the purpose of gating neural prosthetic movements.**

I. Introduction

A number of signals may be derived from intracortically implanted microelectrode arrays for use in a brain-computer interface (BCI). These include manually sorted spike waveforms indicative of single-unit activity (SUA), simple threshold crossings analogous to multi-unit activity (MUA), and the spectral power within specific frequency bands derived from local field potentials (LFPs). The relative information content of these signal modalities has been described previously in the context of both physical reaching movements [1] as well as for decoding the movements of a neural prosthetic device [2], [3].

This work was supported in part by the National Institute of Neurological Disorders and Stroke (NINDS) training grant F32NS092430, NINDS grant R01NS062019, and the Defense Advanced Research Projects Agency (DARPA) grant N66001-10-C-4056.

J.J. Williams is a postdoctoral scholar within the Systems Neuroscience Institute and Center for the Neural Basis of Cognition, University of Pittsburgh, Pittsburgh, PA 15260 USA. (phone: 412-383-5391; fax: 412-383-5460; e-mail: jjw77@pitt.edu).

R.N. Tien is a graduate student within the Department of Bioengineering and Center for the Neural Basis of Cognition, University of Pittsburgh, Pittsburgh, PA 15260 USA. (e-mail: rnt9@pitt.edu).

Y. Inoue is visiting scholar within the Systems Neuroscience Institute, University of Pittsburgh, Pittsburgh, PA 15260 USA. (e-mail: yoceanfive@gmail.com).

A.B. Schwartz is the Distinguished Professor of Neurobiology, University of Pittsburgh, Pittsburgh, PA 15260 USA. (e-mail: abs21@pitt.edu).

While the majority of similar BCI studies have focused on the use of these signals to decode volitional movement kinematics (i.e. movement direction, velocity, etc.), fewer studies have addressed the need to detect when a subject actually desires to control a prosthetic device in the first place. As suggested from our previous work, neural activity recorded during rest between periods of physical reaching movements is often decoded by kinematic firing rate models as a non-zero velocity [4]. Indeed, decoding of this resting state activity by most common BCI algorithms would result in undesired and possibly dangerous prosthetic movements when a subject is resting or distracted. Additionally, inclusion of periods of unintended BCI control could add deleterious noise to movement decoder calibration or other analyses.

To address these needs to eliminate unwanted movements during periods of non-control or remove periods of inattention from analysis, a recent study from our lab demonstrated that an idle state detector based on spiking activity can robustly distinguish periods of rest and appropriately gate the output of a movement decoder [5]. Similarly, an ECoG-based BCI study demonstrated that periods of active BCI control and rest could be accurately classified using epidural field potentials [6]. In the present study, we sought to extend both of these results by examining whether intracortical LFPs may also be used to decipher attention to prosthetic control, and how the utility of these signals compares to that of spiking activity. As has been suggested before, LFP's have been proposed to be a robust BCI signal modality that may be more resistant to degradation over time than spiking activity [2], [3]. Supporting this notion, we present preliminary results that suggest LFP discriminative capacity is on par with that of spiking activity in a frequency specific manner, and population models using either modality are capable of detecting state changes with fine temporal resolution.

II. Methods

A. Behavioral Task

One male rhesus macaque was implanted with two 96-channel intracortical microelectrode arrays (Blackrock Microsystems) in primary motor cortex (M1) of the right hemisphere. The monkey performed a two-dimensional (2D) BCI reaching task using an anthropomorphic robotic arm (WAM Arm, Barrett Technology) while seated comfortably in a primate chair with both arms restrained. The WAM arm was positioned to the left of the monkey and positioned to approximate a "surrogate" left arm contralateral to the implanted arrays. The monkey controlled the end-point

978-1-4577-0220-4/16/$31.00 ©2016 IEEE

velocity of the robotic arm by modulating recorded spiking activity. To begin a trial, a target object attached to the end of a presentation robot (DENSO Robotics) is presented at one of five target locations equally spaced from the WAM arm's starting position in a half-circle configuration ("Present" stage). During target presentation, the WAM arm is automatically held at its starting position. The task then proceeds to the "Reach" phase, where the monkey must move the robot arm (now under active BCI control) toward the target and cross an invisible proximity threshold. After crossing this target radius threshold, the robot arm automatically completes the rest of the movement to grab the target object ("Approach" phase). The interlocked WAM hand and target object with water tube are then driven automatically to the monkey's mouth to deliver a liquid reward ("Drink" phase). Finally, the WAM and DENSO are returned to their home positions before starting the next trial ("Intertrial" phase). Movement of the WAM arm is only influenced by neural signals during the "Reach" phase.

The trial structure above comprises "Active" or "task" trials. We interleaved blocks of "Rest" (or "idle") trials between blocks of "Active" trials to assess potential differences in neural activity between idle and active BCI task states. During "Rest" trials, the target object is returned to its home position away from the monkey, and the WAM arm is locked in place in its home position. Neither robot moves during these trials, and thus provides no motivation for the monkey to modulate neural activity in a task-related manner. Blocks of 10 rest trials lasting approximately 1 minute total were interleaved between every 50 task trials.

B. Data Acquisition and Signal Conditioning

All neural data were recorded using TDT (Tucker Davis Technologies) RZ2 signal acquisition systems. BCI movement control signals were derived from spiking activity (either manually sorted spikes or simple RMS-based threshold crossings). Spiking events were binned into 30 ms bins and used to estimate firing rates using a 15-sample FIR filter with a sample-to-sample exponential decay constant of 0.95. Firing rates were translated to the 2D end-point velocity of the WAM arm using an Optimal Linear Estimator (OLE) model as described in our previous experiments [7]. These estimates of firing rates were also used in all offline analyses described in this report.

In addition to the spiking activity used for online BCI control, LFP waveforms were saved for offline processing and analysis. Raw waveforms were filtered offline using an envelope detection scheme to estimate the spectral power in six frequency bands: 8-15 Hz, 15-24 Hz, 30-50 Hz, 70-90 Hz, 90-110 Hz, and 130-150 Hz. These correspond roughly to classically defined EEG/ECoG bands ('alpha', 'beta', 'low-gamma', and two 'high-gamma' bands), and have been described in ECoG reports of idle-state classification [6]. LFP band amplitude estimates were resampled into 30 ms bins to align with firing rate time-series and smoothed again with the same filter as for firing rates to provide an equal footing for comparison.

C. Training Data

Data used for single-channel analyses and population model training were selected using a subset of trials with the monkey's highest performance based on the assumption that the monkey would be most attentive and motivated during this period. A sliding window of 100 task trials was used to calculate a running average performance over the course of a session. The block of 100 task trials with the highest performance was included in discriminability calculations and classification models. All rest trials within a session were included due to their smaller number and the assumption that attention during these blocks should not fluctuate within the course of a session.

D. Single-Channel Idle State Discriminability

To compare the utility of individual firing rate and LFP features in classifying active/idle states for a BCI task, we employed the discriminability index, *d'*, from signal detection theory [8] using Eq. 1:

$$d' = \frac{\mu_{task} - \mu_{rest}}{\sqrt{p_{task}\sigma_{task}^2 + p_{rest}\sigma_{rest}^2}} \quad (1)$$

$$p_{task} + p_{rest} = 1 \quad (2)$$

where $\mu_{task/rest}$ is the mean firing rate or band amplitude during task and rest periods, $p_{task/rest}$ is the proportion of task and rest samples, and $\sigma_{task/rest}^2$ is the variance in firing rate or band amplitude during those periods. LFP band amplitudes were used to calculate and compare *d'* metrics against corresponding firing rate metrics obtained from the same channel. *d*' values were calculated using trial-binned data where active neural samples were averaged over the reach portion of each trial within the 100 task trial best peak performance window, and rest samples were averaged over the entirety of each rest trial.

E. Population Level Classification

To compare idle/active classification utility at the population level, we built classification models using either only firing rate activity or LFP band activity. For LFP models, all frequency bands on each channel were included. Linear discriminant analysis (LDA) models were trained using "Reach" task samples from the 100-trial peak performance window and all "Rest" samples. LDA models were fit and cross-validated using 10-fold cross-validation.

As the raw output of the population LDA models tested in this study is continuous-valued, the numeric boundary between labeling samples as "idle" or "active" is an arbitrary decision dependent upon desired sensitivity and specificity in detecting those periods. Consequently, a Receiver-Operator Characteristic (ROC) analysis was used to test the classification performance of each model. In this framework, a variable threshold is swept through the range of raw classifier outputs while plotting the corresponding true positive rate vs. false positive rate at each threshold. The resulting Area Under the Curve (AUC) metric (value of 1 indicating perfect classification, 0.5 indicating chance performance) was used to compare performance between models as well as the utility of a given model in discriminating other periods.

F. Classification of Other Non-Reaching Task Periods

The offline models above were trained exclusively on the "Reach" and "Rest" task periods. We also sought to examine

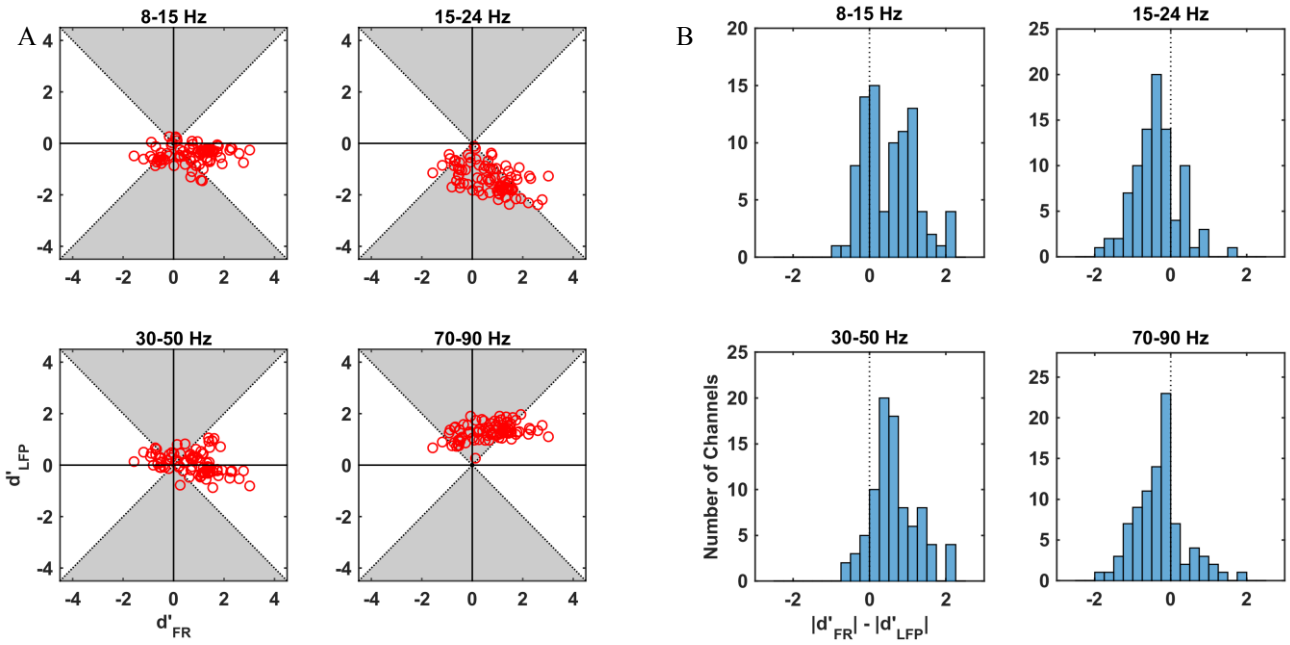

Figure 1. **Comparison of firing rate (FR) and LFP idle/task discriminability, *d'*.** A: *LFP vs. firing rate idle/task discriminability.* Circles indicate the *d'* metrics for an LFP vs. firing rate feature on the same channel. Grey shaded regions indicate channels for which the LFP magnitude of discriminability in a given band was greater than firing rate activity on the same channel, while white regions indicate the opposite relation. B: *Difference in idle/task discriminability for firing rate – LFP.* Histograms derived from panel A show the number of channels with a given difference in magnitude of *d'*. Negative values indicate that the magnitude of the d' for an LFP feature was larger than that calculated from firing rate activity on the same channel.

how these models extend to discriminating other periods of the task from rest. Toward this end, we tested the raw output of these models on other task periods using ROC analysis to identify similarities and differences between the rest/reach states and other task periods.

III. Results

A. Single Channel Discriminability

Fig. 1A depicts the relationship of the *d'* metric (measured in standard deviations, std) for firing rate activity on individual channels versus the LFP activity on the same channel in different frequency ranges (only the first high gamma band is shown for compactness as higher bands displayed similar patterns). As seen from this figure, firing rate activity showed a diverse range of task/rest related modulation both in magnitude ($|d'|$ ranging from near 0 to > 3 std) and sign (both increases and decreases in activity during task relative to rest). Conversely, LFP activity within a given band tended to be more homogenous with a smaller spread in *d'* values than for firing rate activity. Additionally, the sign of modulation was observed to change across bands in a similar pattern to past descriptions of event-related depolarization (ERD) and synchronization (ERS) in both physical movements [9]–[11] and BCI experiments [6].

To assess the relative utility of individual LFP features vs. firing rate activity, we compared the intra-channel difference in the magnitude of *d'* values for those features. As seen from Fig. 1B, a large proportion of LFP features in several frequency bands (15-24 Hz, high gamma bands) held better idle state discriminatory power than their firing rate counterpart on the same channel (channels within the grey shaded regions of Fig. 1A). Conversely, firing rate *d'* metrics tended to be higher than their LFP counterparts in the alpha and low-gamma frequency bands (channels within white regions). Overall, it appears there is useful information for detecting idle/active state changes within single channels in both firing rate and LFP activity. This discriminability capacity is frequency dependent, with beta and high-gamma frequencies often exhibiting higher capacity than same-channel firing rates.

B. Population-level Classification

When models were trained and tested offline on real-time data, performance of both firing rate and LFP models were highly and indistinguishably accurate. Both models achieved an AUC for rest vs. reach samples of over 0.99 and were not significantly different from each other. Any differences observed in single-channel discriminability in Figure 1 appear to have been overcome by the power of averaging over neural features using population-level classification. Fig. 2A depicts a histogram of raw classifier scores produced by an example LFP model for rest, reach, and all task periods as well as the corresponding ROC plots (Fig. 2B). As seen from the figure, the classifier produces good separation between reach and rest distributions with minimal overlap. Firing rate models produced similar separation between states with non-significant differences in performance.

C. Classification of Other Non-Reaching Task Periods

Due to the success in classifying rest and active (reach) periods using either signal modality, we next sought to explore how the performance of these models extended to discriminating rest samples from other periods of the active task. The histograms in Fig. 2A depict the separation in classifier score distributions for the previously mentioned reach and rest samples as well as all active task samples from the peak 100 trial window using an LFP-based model. Fig.

2B breaks down the performance of this model further by ROC analysis of each task period individually vs. rest samples. As seen from the figure, although the classifier was trained exclusively on rest and reach samples, the model extended well to discriminating a majority of active task samples.

Upon closer examination of the time-series of the raw classifier score as shown in Fig. 2C, we noted distinct patterns of raw score modulation correlating with the intra-task structure. Consistent with this observation, ROC analysis of idle scores comparing reach and intertrial periods (both within the active task structure) demonstrated the model still held significant discriminatory capacity at this temporal resolution. Although not as high as for discriminating rest and reach samples, the ROC curve and AUC for reach/intertrial samples were well above random chance (AUC = 0.92).

IV. Discussion

The experiments presented in this preliminary study provide a novel comparison of commonly used intracortical signal modalities, namely firing rate activity and LFPs, for use in detecting rest or active intent to control a prosthetic device in the context of a BCI. Our results suggest that LFPs provide idle/active state discriminability on par with, if not superior to, firing rate activity in a frequency specific manner with beta and high gamma frequencies demonstrating the most promising utility. At a population level, both modalities demonstrated indistinguishably high performance in offline classification of reach and rest states. In addition to the aforementioned potential utility of this classification to gate unwanted prosthetic movements, another application of this result could be to use similar classifiers to throw out entire task trials from further analysis or use in decoder calibration if a subject is distracted from the task. The intra-task state comparisons also suggest that such a classifier scheme may hold utility not only in discriminating obviously different attentional states to the task, but could potentially be used to discriminate discrete states of BCI control within the task itself. Consequently, an appropriate decoder from a predefined set (e.g. reaching, posture, grasping, etc.) could be selected based on the detected state. This state-space approach to BCI decoding has been suggested as a tool to expand the breadth of current BCI control schemes [12], and the results presented here provide promising support for such an approach.

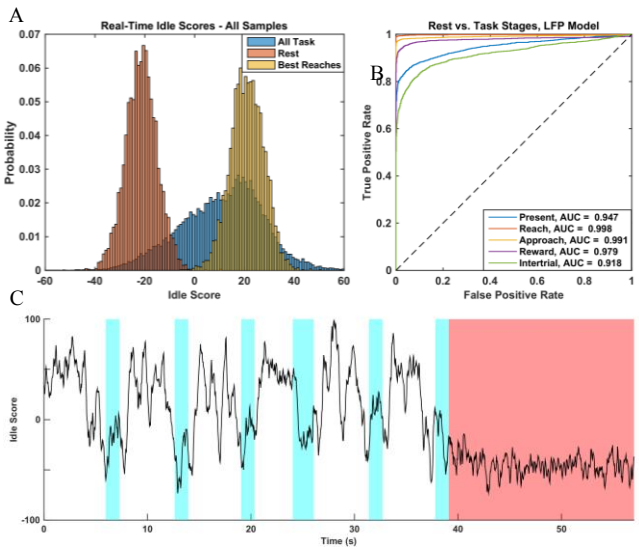

Figure 2. **Real-time discrimination of idle periods vs. all task periods**. Data shown is from an example LFP model. A firing rate model from the same session (results now shown) demonstrated similar results. A: *Histogram of real-time idle score distributions for rest vs. reach or all task samples.* B: *ROC analysis of rest samples vs. individual task periods.* Colored ROC curves indicate classifier performance for a given task period vs. rest with AUC performance metrics shown in the legend. C: *Real-time classifier score evolution during task and rest periods*. Initial white regions indicate the beginning stages of a trial ("Present and "Reach" during which volitional neural modulation is likely. Cyan shaded regions indicate later task stages during which task modulation is not necessary, and correspondingly show a characteristic drop in idle score. The last red region indicates the beginning of a rest period during which the idle score is consistently low.

References

[1] S. Perel, P. T. Sadtler, E. R. Oby, S. I. Ryu, E. C. Tyler-Kabara, A. P. Batista, and S. M. Chase, "Single-unit activity, threshold crossings, and local field potentials in motor cortex differentially encode reach kinematics," *J. Neurophysiol.*, vol. 114, no. 3, pp. 1500–1512, Sep. 2015.

[2] K. So, S. Dangi, A. L. Orsborn, M. C. Gastpar, and J. M. Carmena, "Subject-specific modulation of local field potential spectral power during brain–machine interface control in primates," *J. Neural Eng.*, vol. 11, no. 2, p. 026002, Apr. 2014.

[3] R. D. Flint, Z. A. Wright, M. R. Scheid, and M. W. Slutzky, "Long term, stable brain machine interface performance using local field potentials and multiunit spikes," *J. Neural Eng.*, vol. 10, no. 5, p. 056005, Oct. 2013.

[4] M. Velliste, S. D. Kennedy, A. B. Schwartz, A. S. Whitford, J.-W. Sohn, and A. J. C. McMorland, "Motor Cortical Correlates of Arm Resting in the Context of a Reaching Task and Implications for Prosthetic Control," *J. Neurosci.*, vol. 34, no. 17, pp. 6011–6022, Apr. 2014.

[5] S. B. Suway, R. N. Tien, S. M. Jeffries, Z. Zohny, S. T. Clanton, A. J. McMorland, and M. Velliste, "Resting state detection for gating movement of a neural prosthesis," in *Neural Engineering (NER), 2013 6th International IEEE/EMBS Conference on*, 2013, pp. 665–668.

[6] J. J. Williams, A. G. Rouse, S. Thongpang, J. C. Williams, and D. W. Moran, "Differentiating closed-loop cortical intention from rest: building an asynchronous electrocorticographic BCI.," *J. Neural Eng.*, vol. 10, no. 4, p. 046001, 2013.

[7] J. L. Collinger, B. Wodlinger, J. E. Downey, W. Wang, E. C. Tyler-Kabara, D. J. Weber, A. J. McMorland, M. Velliste, M. L. Boninger, and A. B. Schwartz, "High-performance neuroprosthetic control by an individual with tetraplegia," *The Lancet*, vol. 381, no. 9866, pp. 557–564, Feb. 2013.

[8] D. M. Green, J. A. Swets, and others, *Signal detection theory and psychophysics*, vol. 1974. 1966.

[9] C. Toro, G. Deuschl, R. Thatcher, S. Sato, C. Kufta, and M. Hallett, "Event-related desynchronization and movement-related cortical potentials on the ECoG and EEG," *Electroencephalogr. Clin. Neurophysiol.*, vol. 93, no. 5, pp. 380–389, Oct. 1994.

[10] N. E. Crone, D. L. Miglioretti, B. Gordon, J. M. Sieracki, M. T. Wilson, S. Uematsu, and R. P. Lesser, "Functional mapping of human sensorimotor cortex with electrocorticographic spectral analysis. I. Alpha and beta event-related desynchronization," *Brain J. Neurol.*, vol. 121 (Pt 12), pp. 2271–2299, Dec. 1998.

[11] N. E. Crone, D. L. Miglioretti, B. Gordon, and R. P. Lesser, "Functional mapping of human sensorimotor cortex with electrocorticographic spectral analysis. II. Event-related synchronization in the gamma band," *Brain J. Neurol.*, vol. 121 (Pt 12), pp. 2301–2315, Dec. 1998.

[12] A. G. Rouse and M. H. Schieber, "Advancing brain-machine interfaces: moving beyond linear state space models," *Front. Syst. Neurosci.*, vol. 9, p. 108, 2015.